4304–4312 *Nucleic Acids Research, 1996, Vol. 24, No. 21*

mRNA turnover in yeast promoted by the MATα1 instability element

Giordano Caponigro[+] and Roy Parker[1,*]

Department of Molecular and Cellular Biology and [1]Howard Hughes Medical Institute, University of Arizona, Tucson, AZ 85721, USA

Received June 19, 1996; Revised and Accepted September 5, 1996

ABSTRACT

The decay rates of eukaryotic transcripts can be determined by sequence elements within an mRNA. One example of this phenomenon is the rapid degradation of the yeast MATα1 mRNA, which is promoted by a 65 nt segment of its coding region termed the MATα1 instability element (MIE). The MIE is also capable of destabilizing the stable PGK1 transcript. To determine how the MIE accelerates mRNA turnover we examined the mechanism of degradation of the MATα1 transcript. These experiments indicated that the MATα1 mRNA was degraded by a deadenylation-dependent decapping reaction which exposed the transcript to 5′→3′ exonucleolytic digestion. Deletion of the MIE from the MATα1 mRNA decreased the rate at which this mRNA was decapped. In contrast, insertion of the MIE into the PGK1 transcript caused an increase in the rate of deadenylation of the resulting chimeric mRNA. These observations suggest that the MIE promotes rapid mRNA decay by increasing the rates of deadenylation and decapping, with its primary effect on mRNA turnover depending on additional features of a given transcript. These results also strengthen the hypothesis that deadenylation-dependent decapping is a common pathway of mRNA decay in yeast and indicate that an instability element within the coding region of an mRNA can effect nucleolytic events that occur at both the 5′- and 3′-ends of an mRNA.

INTRODUCTION

The rate at which an mRNA decays influences both its steady-state level and the time required for a maximal change in its level following a change in its rate of synthesis (for a discussion see 1). Given this influence, knowledge of how the decay rates of individual mRNAs are specified is critical to understanding the control of gene expression. A basis for differences in mRNA decay rates has come from a set of observations indicating that mRNA half-lives are influenced by discrete sequences within mRNAs that serve to either destabilize or stabilize transcripts. Such sequences have been identified in the 5′-untranslated regions (UTRs), coding regions and 3′-UTRs of various eukaryotic mRNAs (for reviews see 2–4). In a few cases experimental evidence has suggested possible mechanisms by which 'instability' elements may function to promote mRNA decay. For example, portions of the mammalian c-*fos* mRNA 3′-UTR and coding region and the 3′-UTR of the yeast MFA2 transcript appear to promote mRNA turnover by increasing rates of deadenylation (5–11). Alternatively, sequence elements within several other transcripts from higher eukaryotes promote mRNA turnover by functioning as specific endonuclease cleavage sites (12–16). However, further study of many of these instability elements has been limited in the absence of either a useful genetic approach or a knowledge of the complete mRNA turnover pathway.

The simple eukaryote *Saccharomyces cerevisiae* provides an excellent system for determining how sequence elements influence mRNA degradation. Several different mechanisms of mRNA decay have been extensively characterized in yeast, including deadenylation-dependent decapping, deadenylation-independent decapping and 3′→5′ pathways of mRNA decay (8,17–19). Knowledge of these different mechanisms of degradation allows analysis of whether instability elements promote mRNA degradation through these established pathways or through other pathways of decay. In addition, the powerful genetic tools available in yeast should facilitate the identification and subsequent analysis of *trans*-acting factors that mediate the effects of sequence elements influencing mRNA decay.

One well-defined instability element from yeast is a 65 nt segment of the MATα1 mRNA coding region, termed the MATα1 instability element (MIE). The MIE is both necessary for rapid turnover of the MATα1 transcript ($t_{1/2}$ = 3.5 min) and sufficient to accelerate decay of the stable PGK1 transcript (20). Several observations suggest that the ability of this element to stimulate mRNA degradation is dependent on translation. The MIE is located in the coding region of the MATα1 mRNA and translation up to or through this element is required for it to promote rapid mRNA decay (21,22). Furthermore, this element contains a run of several rare codons in the 5′ 33 nt which, while unable to promote decay themselves, stimulate decay mediated by the 3′ 32 nt (20). Thus, translation and rapid mRNA degradation mediated by this element may be linked through ribosomal pausing at a specific region on the mRNA (20). Given these observations, determining how the MIE functions as an instability element is likely to provide insight into how mRNA translation and decay are coupled.

*To whom correspondence should be addressed. Tel: +1 520 621 3442; Fax: +1 520 621 4524; Email: parker-lab@tikal.biosci.arizona.edu

[+]Present address: Ventana Genetics Inc., 807 E. South Temple, Suite 310, Salt Lake City, UT 84102, USA

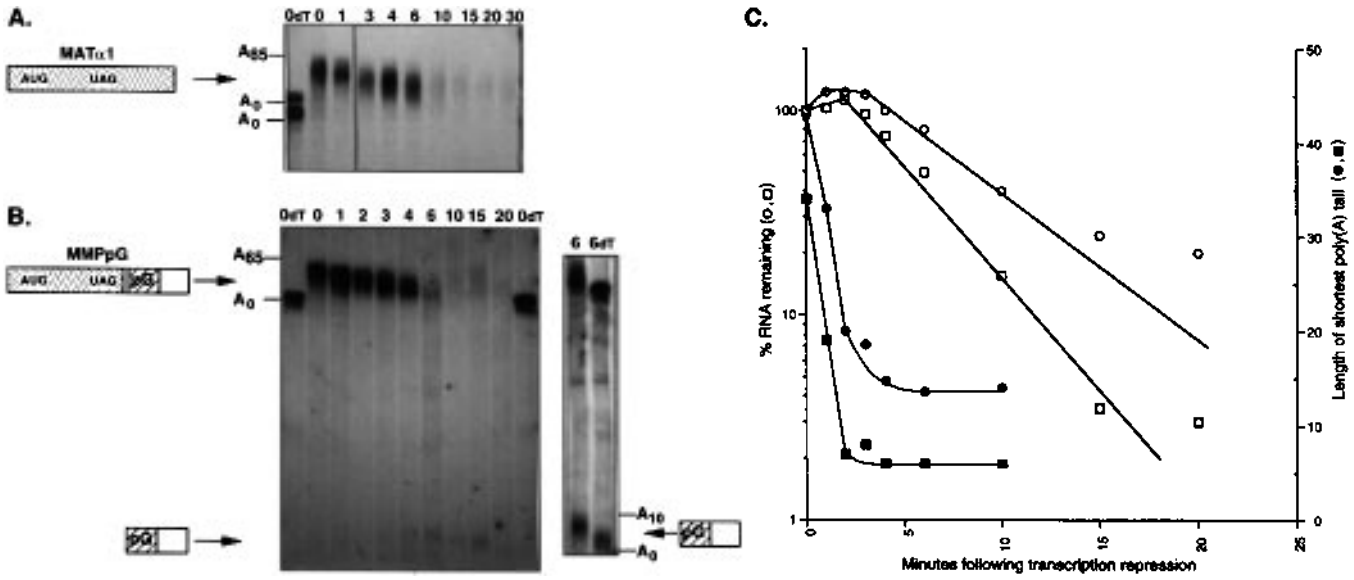

Figure 1. Deadenylation precedes degradation of the MATα1 mRNA. Shown are transcriptional pulse-chase experiments examining decay of the (**A**) MATα1 and (**B**) MMPpG mRNAs. Minutes following transcription repression are shown above and poly(A) tail lengths are shown to the left of each panel. In these and all subsequent figures, poly(A) tail lengths were determined by comparison with the oligo(dT)-treated samples and size standards (see Materials and Methods and data not shown). Schematic representations of each RNA species are shown to the right of each panel. Shaded regions represent MATα1 sequences and open regions represent PGK1 sequences. Hash-marked areas marked with pG show the location of the poly(G) insertion. (B insert) Shown is 3-fold more RNA from the 6 min time point from (B) either plus (6dT) or minus (6) treatment with RNase H and oligo(dT). Poly(A) tail lengths on and a schematic of the decay intermediate are shown to the right of the panel. The probes used to detect the MATα1 transcript in (A) was a random primed DNA *Sca*I–*Hin*dIII fragment which spans the MATα1 3′-UTR. The probe used to detect the MMPpG transcripts in (B) and (B insert) was a 5′-end-labeled oligonucleotide (oRP121) complementary to the poly(G) tract respectively (see Materials and Methods). (**C**) Graph depicting the deadenylation and degradation of the MATα1 and MMPpG mRNAs in transcriptional pulse-chase experiments. The upper two curves represent the decay of the (○) MATα1 and (□) MMPpG mRNAs. The lower two curves represent the lengths of the shortest poly(A) tails on the (●) MATα1 and (■) MMPpG mRNAs. Each data point is the average of multiple experiments. In these experiments differences in RNA levels resulting from unequal handling of samples were controlled for by stripping blots and reprobing with an oligonucleotide probe complementary to the ScR1 transcript as described (8).

In this work we analyzed how the MIE stimulates decay of both the MATα1 and PGK1 mRNAs. These studies indicate that the MIE influences decay of the MATα1 mRNA by increasing the rate at which this mRNA is decapped and stimulates turnover of the PGK1 transcript by increasing its rate of deadenylation. Thus an instability element located in the coding region of an mRNA can influence nucleolytic events that occur at both the 5′- and 3′-ends of mRNAs. Knowledge of how the MIE affects mRNA turnover will allow future studies of the specific *trans*-acting factors that mediate the effects of this instability element.

MATERIALS AND METHODS

Strains and media

In the experiments described in Figures 1, 3 and 5 the yeast strain used was yRP582 (MAT**a**, *rpb1-1*, *ura3-52*, *leu2-3*, *112*; 8). The plasmids contained in this strain in the various experiments were as follows: Figure 1, either pRP631 (pGAL-MATα1; 20) or pRP702 (pGAL-MMPpG; see below); Figure 3, either pRP633 (pGAL-MATα1.$\Delta^{182–339}$; 20) or pRP703 (pGAL-MMPpG.$\Delta^{182–339}$; see below); Figure 5, either pRP139 (pGAL-PαP.0; see below), pRP141 (pGAL-PαP.201–351; see below) or pRP142 (pGAL-PαP.201–266; see below). pRP139, 141 and 142 are identical to plasmids PαP.0, PαP.201–266 and PαP.201–351 (described in 20), except that in each case the chimeric genes have been placed under the regulation of the GAL1 UAS. Yeast strains examined in Figures 2 and 4 were yRP689 (MAT**a**, *rpb1-1*, *ura3-52*, *leu2-3*, *112*, *xrn1*::*URA3*; 17), yRP1108 (MAT**a**, *rpb1-1*, *ura3-52*, *leu2-3*, *112*, *trp1-Δ1*, *lys2-201*, *dcp1*::*URA3*; 23) and yRP1117 (MAT**a**, *rpb1-1*, *ura3-52*, *leu2-3*, *112*). These yeast strains contained plasmid pRP704 (see below) in the experiments shown in Figure 2 and plasmid pRP744 (see below) in the experiments shown in Figure 4. pRP704 contains the MATα1 gene under the control of the GAL1 UAS and pRP744 contains the MATα1.$\Delta^{182–339}$ gene

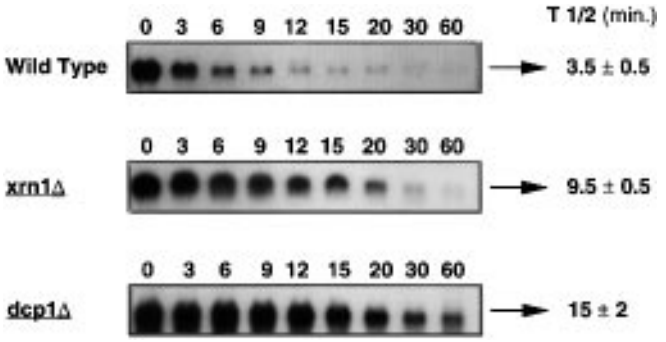

Figure 2. Degradation of the MATα1 mRNA in cells lacking either the *XRN1* or *DCP1* gene products. (**A**) Decay of the MATα1 mRNA from steady-state in wild-type, *xrn1*Δ and *dcp1*Δ cells (see Materials and Methods). Relevant genotypes of the strains are shown to the left, minutes following transcription repression are shown above and half-lives are shown to the right of each panel. Strains used in this study were yRP689 (*xrn1*Δ), yRP1108 (*dcp1*Δ) and yRP1117 (wild-type, see Materials and Methods). Differences in RNA levels resulting from unequal handling of samples were controlled for as described in the legend to Figure 1.

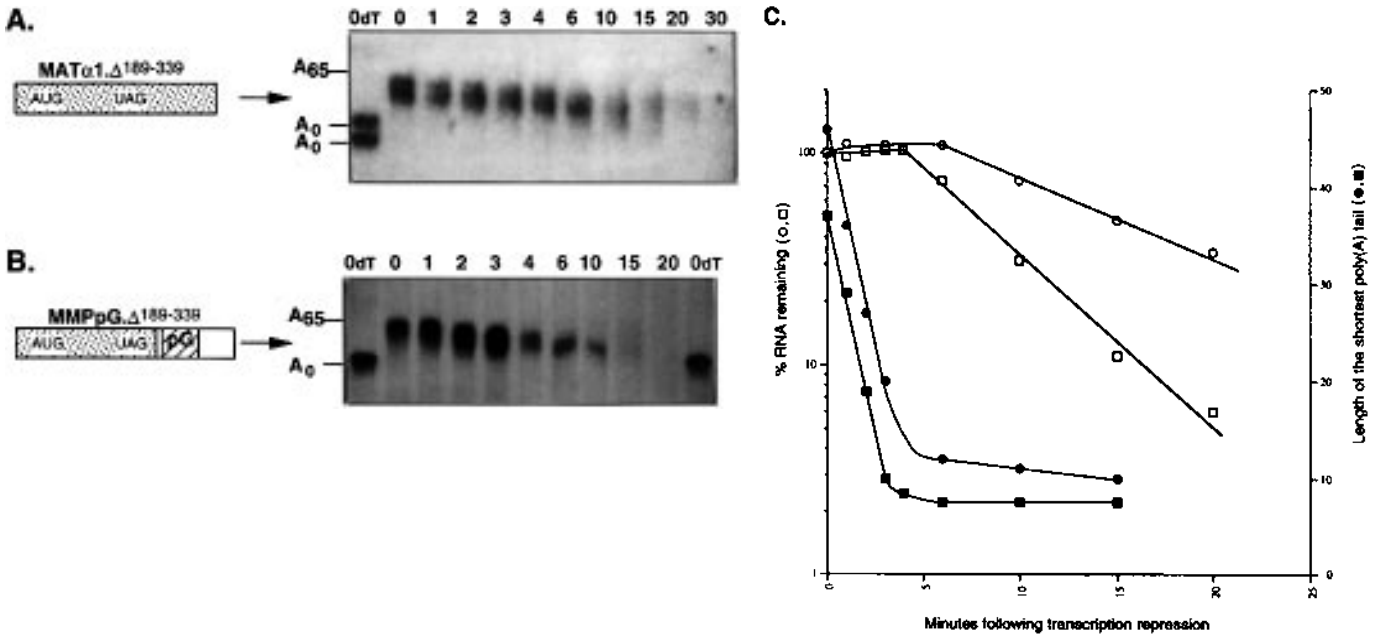

Figure 3. Deletion of the MIE slows mRNA degradation following deadenylation. Shown are transcriptional pulse-chase experiments examining decay of the (**A**) MATα1.$\Delta^{189–339}$ and (**B**) MMPpG.$\Delta^{189–339}$ mRNAs. Poly(A) tail lengths and schematics of each mRNA are shown to the left of the panels. As before, shaded regions represent MATα1 sequences, open regions represent PGK1 sequences and the hash-marked region marked with pG shows the location of the poly(G) insertion. Probes used to detect the MATα1.$\Delta^{189–339}$ and MMPpG.$\Delta^{189–339}$ mRNAs were as described in Figure 1. (**C**) Graph depicting deadenylation and degradation of the MATα1.$\Delta^{189–339}$ and MMPpG.$\Delta^{189–339}$ mRNAs in transcriptional pulse-chase experiments. The upper two curves represent decay of the (○) MATα1.$\Delta^{189–339}$ and (□) MMPpG.$\Delta^{189–339}$ mRNAs. The lower two curves represent the lengths of the shortest poly(A) tails on the (●) MATα1.$\Delta^{189–339}$ and (■) MMPpG.$\Delta^{189–339}$ mRNAs. Each data point is the average of multiple experiments. Differences in RNA levels resulting from unequal handling of samples were controlled for as described in the legend to Figure 1.

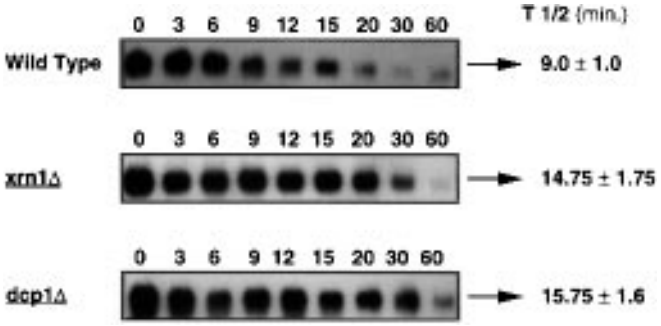

Figure 4. Degradation of the MATα1.$\Delta^{189–339}$ mRNA in cells lacking either the *XRN1* or *DCP1* gene products. (**A**) Decay of the MATα1.$\Delta^{189–339}$ mRNA from steady-state in wild-type, *xrn1*Δ and *dcp1*Δ cells (see Materials and Methods). Relevant genotypes of the strains are shown to the left, minutes following transcription repression are shown above and half-lives are shown to the right of each panel. Differences in RNA levels resulting from unequal handling of samples were controlled for as described in the legend to Figure 1.

under the control of the GAL1 UAS. Decay of the MATα1 and MATα1.$\Delta^{182–339}$ mRNAs were determined following a simultaneous shift from 24 to 36°C and glucose repression as described elsewhere (20). Appropriate selections were used to maintain plasmids introduced by transformation.

Plasmid constructions

pRP702 (pGAL–NMppG) construction. pRP129, which contains the entire PGK1 gene, was digested with *Cla*I, filled with Klenow enzyme and *Bgl*II linkers (New England Biolabs #1001) were ligated to the blunt ends. The construct was then digested with *Bgl*II and ligated to oRP126 and 127 (5′-GATCTAGGAATTTGG-GGGGGGGGGGGGGGGGAATTCCT-3′ and 5′-GATCAGGA-ATTCCCCCCCCCCCCCCCCCCAAATTCCT- A-3′ respectively; 8). A construct containing a single oRP126/127 insertion was then cut with *Bgl*II, filled with Klenow enzyme and cut with *Bam*HI. A resulting fragment containing the 3′-UTR of PGK1 and vector sequences was ligated to an ~1 kb *Bam*HI–*Sca*I fragment from pRP631 (pGAL-MATα1; 20) which contained the MATα1 5′-UTR, coding region and first 35 nt of the 3′-UTR. The resulting construct was digested with *Bam*HI and *Eco*RI and ligated to an ~750 nt *Bam*HI–*Eco*RI fragment from pRP631 that contained the GAL1 UAS, creating pRP702 (pGAL-MMPpG). pRP703 (pGAL-MMPpG.$\Delta^{182–339}$) was constructed in an identical manner to pRP702 except that the *Bam*HI–*Sca*I fragment was isolated from pRP633 (pGAL-MATα1.$\Delta^{182–339}$; see 20) instead of pRP631.

To allow selection of plasmids carrying the pGAL-MATα1 and pGAL-MATα1.$\Delta^{182–339}$ genes in yRP689, yRP1108 and yRP1117, plasmids pRP704 and pRP744 were constructed. The *LEU2* gene was first isolated on a *Nar*I (filled)–*Hin*dIII fragment and ligated to pRP633 which had been digested with *Nar*I, filled with Klenow enzyme and digested with *Hin*dIII, creating pRP744. The resulting plasmid was digested with *Bam*HI and *Hin*dIII and the fragment containing vector and GAL1 UAS sequences was ligated to a *Bam*HI–*Hin*dIII fragment from pRP631 that contained MATα1 5′-UTR, coding region and 3′-UTR sequences, creating pRP704.

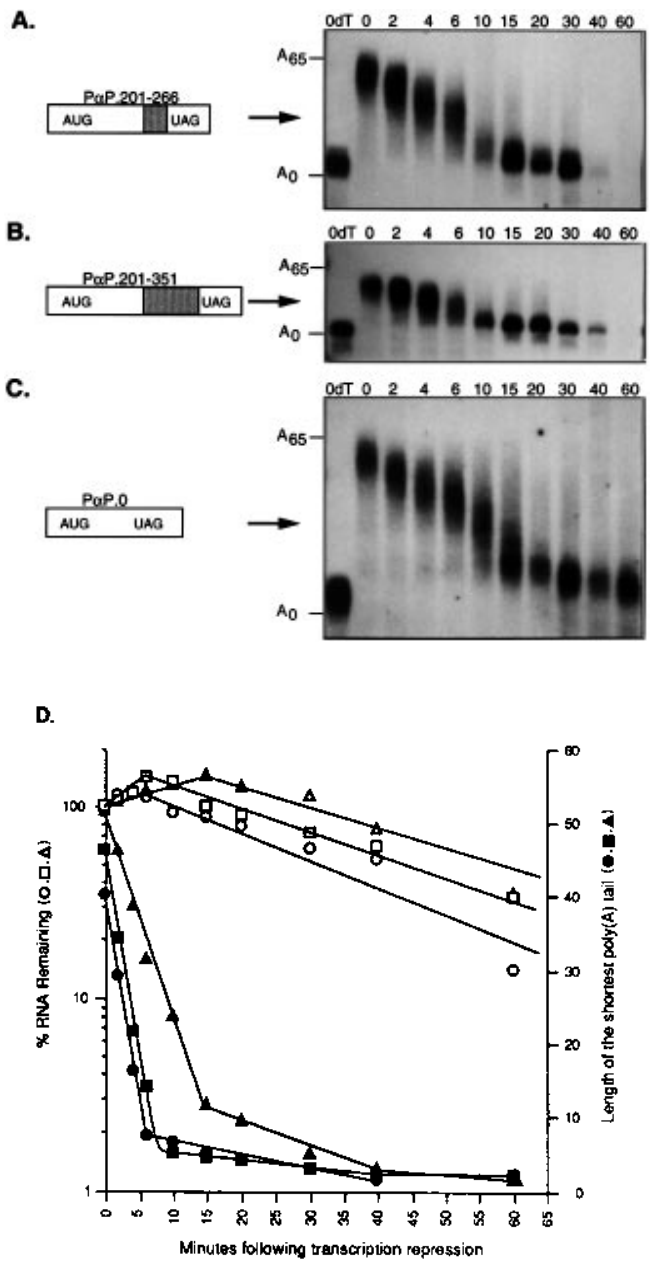

Figure 5. The MIE increases the rate of deadenylation of PGK1 mRNA. Shown are transcriptional pulse-chase experiments examining decay of the (**A**) PαP.201–266, (**B**) PαP.201–351 and (**C**) PαP.0 mRNAs. These mRNAs contain 65 (the MIE), 150 (the MIE and an additional 85 3′ nt) and 0 nt of the MATα1 mRNA fused in-frame to the PGK1 transcript (see 20). Minutes following transcription repression are shown above and poly(A) tail lengths as well as schematics of the mRNAs to the left of each panel. Shaded areas represent MATα1 sequences and open regions represent PGK1 sequences; schematics are not drawn to scale. (**D**) Graph depicting deadenylation and degradation of the PαP.201–266, PαP.201–351 and PαP.0 mRNAs in transcriptional pulse-chase experiments. The upper three curves represent decay of the (□) PαP.201–266, (○) PαP.201–351 and (Δ) PαP.0 mRNAs. The lower two curves represent the lengths of the shortest poly(A) tails on the (■) PαP.201–266, (●) PαP.201–351 and (▲) PαP.0 mRNAs. Each data point is the average of multiple experiments. Differences in RNA levels resulting from unequal handling of samples were controlled for as described in the legend to Figure 1.

RNA methodology

Transcription repression and RNA isolation, quantification and standardization were performed as described previously (20) with the following exception. RNA levels in Northern blots performed in strains yRP1108 and 1117 were quantified using a Phosphorimager (Molecular Dynamics) instead of a Betascope (Betagen). Transcriptional pulse-chase experiments were performed as described previously (8). Where mentioned, rates of poly(A) shortening were determined by measuring the change in length with time of the shortest mRNA species in total poly(A) populations. Where mentioned, rates of degradation following deadenylation were determined by measuring loss of total mRNA with time once decay commenced in transcriptional pulse-chase experiments. In Figures 1 and 3 the MATα1, MMPpG, MATα1.$\Delta^{182–339}$ and MMPpG.$\Delta^{182–339}$ mRNAs were cleaved with RNase H and an oligonucleotide, oRP57 (5′-ATTTTG-TCCGCGTGCCAT-3′), which is complementary to nt 367–383 of the coding region of the MATα1 transcript, prior to loading on the gel. The probe used to detect the MATα1 and MATα1.$\Delta^{182–339}$ mRNAs in Figures 1–4 was a random primed *Sca*I–*Hin*dIII DNA fragment that spanned the MATα1 3′-UTR. The probe used to detect the MMPpG and MMPpG.$\Delta^{182–339}$ mRNAs in Figures 1 and 3 (except where specifically noted; see text) was a 5′-end-labeled oligonucleotide, oRP121 (5′-AATTCCCCCCCCCCCCCCCC-CCA-3′), which is complementary to the poly(G) tract within these mRNAs. In Figure 4 the PαP.0 mRNA was cleaved 190 nt upstream of its major 3′-end with RNase H and an oligonucleotide, oRP26 (5′-TCTATCGATCTACTCGAGGATCT-3′), which spans the junction between the PGK1 coding region and 3′-UTR, prior to loading on the gel. The PαP.201–266 and PαP.201–351 mRNAs were cleaved 187 and 272 nt upstream of their major 3′-ends respectively with RNase H and an oligonucleotide, oRP23 (5′-GTCGAAACT-GAGTATTTTGACTTCCAGACGCTATCC-3′), which is complementary to MATα1 sequences present in both of these chimeric transcripts, prior to loading on the gel. The probe used to detect the PαP.0, PαP.201–266 and PαP.201–351 mRNAs was a 5′-end-labeled oligonucleotide, oRP25 (5′-TTAGCGTAAAGGAT-GGGG-3′), which is complementary to a region within the PGK1 3′UTR.

RESULTS

Deadenylation precedes decay of the MATα1 transcript

In order to understand how the MIE accelerates decay of the MATα1 transcript it was necessary to first define the pathway through which the MATα1 mRNA is degraded. Deadenylation is the first step in the decay of several yeast and mammalian transcripts (6,8,10,11,24). To determine if deadenylation was the first step in the decay of the MATα1 mRNA we examined the turnover of this transcript in a transcriptional pulse-chase experiment (8). In a transcriptional pulse-chase, transcription from a GAL1-regulated gene is induced by shifting cells growing in raffinose containing medium to medium containing galactose. Following a brief induction (8 min) transcription is rapidly shut off by simultaneous glucose repression and thermal inactivation of a temperature-sensitive allele of RNA polymerase II. The short period of mRNA synthesis creates a synchronously produced pool of transcripts which can then be monitored for both deadenylation and decay following transcription repression. This technique has proven useful for the study of mRNAs which are

Table 1. Rates of deadenylation and degradation of mRNAs examined

mRNA	Strain[a]	Steady state half-life[b]	Length of oligo(A) tail[c]	Deadenylation rate[d]	Approximate half-life following deadenylation[e]
MATα1	Wild Type	3.5 ± 0.5	17 ± 4	9 ± 3	4 ± 1
MATα1	xrn1Δ	9.5 ± 0.5			
MATα1	dcp1Δ	15 ± 2			
MATα1.Δ$^{182-339}$	Wild Type	9.0 ± 1	13 ± 6	8.5 ± 3	9 ± 1
MATα1.Δ$^{182-339}$	xrn1Δ	14.75 ± 1.75			
MATα1.Δ$^{182-339}$	dcp1Δ	15.75 ± 1.6			
MMPpG	Wild Type	2.5 ± 0.5	6 ± 2	13 ± 2	2.5 ± 0.5
MMPpG.Δ$^{182-339}$	Wild Type	6 ± 1	10 ± 2	10 ± 2	5 ± 1
PαP.201-266	Wild Type	10 ± 0.5	13 ± 1	6 ± 0.5	32 ± 7
PαP.201-351	Wild Type	10 ± 0.5	11 ± 1	7 ± 1	26 ± 4
PαP.0	Wild Type	29 ± 1	10 ± 1	3 ± 0.5	32 ± 5

[a]Strain designations are as follows; yRP1117 (Wild type), yRP689 (*xrn1*Δ), yRP1108 (dcp1Δ).
[b]Steady-state half-lives in minutes as determined previously, or in this study (see text and Materials and Methods.
[c]Length of the shortest poly(A) tails in nucleotides at the time when decay of the body of the transcript started.
[d]Change in the length of the shortest poly(A) tails with time until oligo(A) length poly(A) tails were attained, expressed in nucleotides per minute.
[e]mRNA decay rates following the initial temporal lag in transcriptional pulse-chase experiments, expressed in minutes.

degraded by both deadenylation-dependent and deadenylation-independent mechanisms (8,17–19). If deadenylation precedes decay of the MATα1 transcript then there should be a temporal lag prior to decay of the body of this mRNA corresponding to the time required to shorten its poly(A) tail (8), whereas no such lag should be observed if this mRNA degrades through a deadenylation-independent pathway of mRNA decay (8).

A transcriptional pulse-chase experiment examining the decay of the MATα1 mRNA is shown in Figure 1A. The key observation is that there was a lag of 4 min prior to decay of the MATα1 mRNA following transcription repression. During this lag the poly(A) tail of this mRNA was shortened to an oligo(A) length of 17 ± 4 nt (Fig. 1C and Table 1), as determined by comparing the lengths of the shortest poly(A) tailed species in the total population to an mRNA sample that had been treated with RNase H and oligo(dT) to remove the poly(A) tail (0dT lane) and size standards (data not shown). Shortening of this mRNA with time was due to loss of the poly(A) tail rather than trimming of the transcript from the 5′-end, since the MATα1 mRNA was cleaved 342 nt 5′ of the major 3′-end prior to loading on the gel by treatment with RNase H and an oligonucleotide (see Materials and Methods) and therefore had common 5′-ends. It should be noted that because the MATα1 transcript was predominantly polyadenylated at two closely spaced 3′-ends precise measurements of poly(A) tail lengths were difficult to obtain [lengths of the shortest poly(A) tails were determined from the shorter of the two ends]. However, the fact that the MATα1 transcript did not become a substrate for decay until the poly(A) tails of some of the total transcripts had shortened to an oligo(A) length suggests that deadenylation precedes degradation of the body of the MATα1 mRNA.

To further investigate whether deadenylation precedes decay of the MATα1 mRNA a poly(G) tract was introduced into the MATα1 mRNA. This was accomplished by replacing the 3′-UTR of the MATα1 mRNA with the 3′-UTR of the PGK1 mRNA, which also contains a poly(G) tract, creating a chimeric mRNA termed MMPpG ($t_{1/2}$ = 2.5 ± 0.5 min; Table 1). Insertion of a poly(G) tract, which forms a stable secondary structure capable of blocking exonucleases *in vitro* (25–27), into the yeast MFA2 and PGK1 mRNAs results in the accumulation of decay intermediates that arise from 5′→3′ digestion of these transcripts (8,17,19,28). In transcriptional pulse-chase experiments examining the decay of the MFA2 and PGK1 mRNAs, 5′→3′ decay intermediates were produced only following deadenylation of the full-length transcripts and had oligo(A) length poly(A) tails, indicating that deadenylation preceded decay (8). Thus, the timing of production and length of poly(A) tails on 5′→3′ decay intermediates can be used to determine whether deadenylation precedes the decay of an mRNA.

A transcriptional pulse-chase experiment examining the MMPpG mRNA is shown in Figure 1B. Several observations strongly suggest that deadenylation precedes the decay of the MMPpG mRNA. First, decay of the MMPpG mRNA commenced 3 ± 1 min following transcription repression, during which time the poly(A) tail was shortened to an oligo(A) length of 6 ± 2 nt (Fig. 1C and Table 1, determined as in Fig. 1A). Second, concomitant with decay of the full-length mRNA a mRNA species corresponding in size to a MMPpG decay intermediate trimmed to the 5′-side of the poly(G) insertion began to accumulate (Fig. 1B). This mRNA species could be detected with an oligonucleotide probe complementary to a region 40 nt 3′ of the poly(G) insertion, but not with a probe complementary to a region 42 nt 5′ of the poly(G) insertion (data not shown), indicating that it was shortened either to, or very near to, the 5′-end of the poly(G) tract. This mRNA species also showed a precursor–product relationship with the full-length mRNA, as it first appeared at 4 min and reached maximum levels at 6–10 min following transcription repression. These observations strongly suggest that this mRNA species was a decay intermediate of the full-length mRNA. Importantly, this mRNA species had only a short poly(A) tail as determined by treatment with RNase H and oligo(dT) (Fig. 1B, inset), indicating that it was produced from deadenylated full-length transcripts. We interpreted these observations to indicate that decay of the MMPpG mRNA occurs only after the poly(A) tail of the mRNA has been shortened to an oligo(A) length.

The MATα1 mRNA is decapped and degraded in a 5′→3′ direction

The previous observation that 5′→3′ decay intermediates are generated from the MMPpG mRNA indicated that this mRNA is degraded via 5′→3′ exonucleolytic digestion. However, it could not be determined whether 5′→3′ digestion of this mRNA was initiated following endonucleolytic cleavage within the body of the mRNA or following decapping of the mRNA by cleavage near its 5′-end, as has been observed for the MFA2 and PGK1 mRNAs (17,19). One useful method for determining whether a transcript is degraded by decapping and/or 5′→3′ digestion is to take advantage of mutants impaired in their capacity to either decap or exonucleolytically digest mRNAs. For instance, stabilization of a transcript in a mutant strain unable to decap mRNAs would indicate that the mRNA was degraded through a mechanism involving decapping. In yeast, decapping of many mRNAs is carried out by the product of the *DCP1* gene (23). Following decapping, 5′→3′ digestion of many mRNAs is performed by the product of the *XRN1* gene, which encodes a major cytoplasmic 5′→3′ exonuclease (29–31). To determine whether the MATα1 transcript is degraded by decapping and subsequent 5′→3′ exonucleolytic digestion, the half-life of this mRNA was examined in *xrn1*Δ and *dcp1*Δ yeast strains (see Materials and Methods).

To measure the half-life of the MATα1 mRNA, wild type, *xrn1*Δ and *dcp1*Δ yeast strains, which also contained the *rpb1-1* mutation, a temperature-sensitive lesion in the gene encoding RNA polymerase II, were grown at 24°C to mid-log phase in medium which contained a mixture of 2% galactose and 2% sucrose to induce production of the MATα1 mRNA from a plasmid carrying a GAL1 UAS-regulated MATα1 gene. RNA was then isolated at various times following a block to transcription imposed by simultaneously shifting cells from 24 to 36°C and adding glucose to the medium (see Materials and Methods). In good agreement with previous measurements (20), the MATα1 transcript degraded with a half-life of 3.5 ± 0.5 min in the wild-type strain (Fig. 2). In contrast, this mRNA was stabilized ~3- and 4-fold in *xrn1*Δ and *dcp1*Δ cells respectively (Fig. 2 and Table 1). The fact that the MATα1 mRNA was stabilized in yeast mutants impaired in their ability to either decap or exonucleolytically degrade mRNAs in a 5′→3′ direction following decapping argued strongly that the MATα1 mRNA is degraded by decapping and subsequent 5′→3′ exonucleolytic digestion.

It should be noted that the MATα1 mRNA was stabilized to a greater extent in the *dcp1*Δ than the *xrn1*Δ strain (15 versus 9.5 min). One likely reason as to why this difference exists is that there may be additional 5′→3′ exonucleases that can partially compensate for the loss of Xrn1p, but no additional decapping activities that can compensate for the loss of Dcp1p. Support for this model comes from several observations. The PGK1 mRNA is subject to low levels of 5′→3′ digestion even in the absence of Xrn1p, indicating that there are additional 5′→3′ exonucleases that can degrade mRNAs (18,19). Furthermore, a second 5′→3′ exonuclease encoded by the *RAT1*/*HKE1* gene has been identified, although the role of this exonuclease in mRNA degradation is unclear (32,33). In contrast, in the absence of Dcp1p there are no detectable 5′→3′ decay intermediates produced from either the MFA2 or PGK1 transcripts, suggesting that there are no additional decapping proteins (23). Moreover, no biochemically similar decapping activities are detected in cell-free extracts generated from *dcp1*Δ yeast (23).

The MIE increases the rate at which the MATα1 transcript degrades following deadenylation

Given the mechanism of MATα1 mRNA degradation it is likely that the MIE stimulates decay of the MATα1 transcript by increasing either the rate at which this mRNA is deadenylated or degraded following deadenylation. To investigate these possibilities we compared the rates of both deadenylation and degradation following deadenylation of mRNAs containing and lacking the MIE using the transcriptional pulse-chase technique. The first of two mRNA pairs examined was the MATα1 transcript and a similar transcript termed MATα1.$\Delta^{182–339}$, which contains an in-frame deletion of the MIE and an additional 74 nt 3′ of the MIE ($t_{1/2}$ = 9 min; Table 1; 20). The additional 74 nt were included in this deletion because this region of the mRNA contains sequences that are functionally redundant to the MIE and can therefore partially compensate for its loss (20). The second pair examined was the MMPpG mRNA (Fig. 1B) and a similar transcript, termed MMPpG.$\Delta^{182–339}$ ($t_{1/2}$ = 6 min; Table 1; see Materials and Methods), which contains a coding region deletion identical to that described for the MATα1.$\Delta^{182–339}$ mRNA.

Transcriptional pulse-chase experiments examining the MATα1.$\Delta^{182–339}$ and MMPpG.$\Delta^{182–339}$ mRNAs are shown in Figure 3A and B. In both cases deletion of the MIE decreased the degradation rate of the oligo(A) form of the mRNA relative to mRNAs containing the MIE, but did not greatly affect rates of deadenylation. The MATα1.$\Delta^{182–339}$ transcript was deadenylated at a rate of 8.5 ± 3 nt/min, very similar to the rate determined for the MATα1 transcript (9 ± 3 nt/min; Fig. 1C and Table 1). However, the approximate half-life of the MATα1.$\Delta^{182–339}$ mRNA following deadenylation was 9 ± 1 min, as opposed to 4 ± 1 min for the MATα1 mRNA (Table 1 and compare Figs 1C and 3C). In addition, while the deadenylation rates of the MMPpG.$\Delta^{182–339}$ and MMPpG mRNAs were similar (10 ± 2 versus 13 ± 1 nt/min respectively; Table 1), the MMPpG.$\Delta^{182–339}$ mRNA degraded 2-fold more slowly following deadenylation than did the MMPpG transcript (Table 1). These results indicate that the MIE primarily effects degradation of the MATα1 mRNA by accelerating the rate at which this mRNA was degraded following deadenylation.

The MIE stimulates decapping of the MATα1 mRNA

The MIE could stimulate degradation of the MATα1 mRNA following deadenylation by increasing the rates of decapping and/or 5′→3′ exonucleolytic digestion. To distinguish between these possibilities we again took advantage of the *dcp1*Δ and *xrn1*Δ mutant strains, which are impaired in their capacity to decap and exonucleolytically digest mRNAs respectively (17,23,30,34). If an instability element stimulates mRNA decay by increasing the rate of a particular nucleolytic event, then the effect of that element on mRNA degradation should be lost in the absence of the protein that performs the nucleolytic event. For instance, if the MIE increased the rate of decapping then the MATα1 and MATα1.$\Delta^{182–339}$ mRNAs should degrade at the same rate in the absence of Dcp1p. Alternatively, if the MIE increased the rate of 5′→3′ exonucleolytic digestion then the MATα1 and MATα1.$\Delta^{182–339}$ mRNAs should degrade at the same rate in an *xrn1*Δ strain.

The half-life of the MATα1.$\Delta^{182–339}$ mRNA was determined in wild-type, *xrn1*Δ and *dcp1*Δ yeast as previously described for the MATα1 mRNA. In close agreement with previous results

(20), the MATα1.Δ$^{182–339}$ transcript was more stable in the wild-type strain than was the MATα1 mRNA, degrading with a half-life of 9 as compared with 3.5 min (compare Figs 2 and 4). Similarly, in the *xrn1*Δ strain the MATα1.Δ$^{182–339}$ RNA was stabilized relative to the MATα1 mRNA, degrading with a half-life of 14.75 ± 1.75 as compared with 9.5 ± 0.5 min (Figs 2 and 4). The fact that the MATα1 mRNA was stabilized following removal of the MIE in the *xrn1*Δ strain indicates that the MIE does not stimulate mRNA degradation by increasing the rate of 5′→3′ decay performed by Xrn1p. In contrast, the MATα1.Δ$^{182–339}$ and MATα1 mRNAs degraded with similar half-lives in wild-type and *dcp1*Δ strains (15.75 ± 1.6 and 15 ± 2 min respectively; Figs 2 and 4). Thus, the MIE has no effect on degradation of the MATα1 mRNA in the absence of Dcp1p, indicating that it stimulates mRNA degradation by increasing the rate of mRNA decapping. Based on these observations we conclude that the MIE increases the rate at which the MATα1 mRNA degrades following deadenylation by stimulating the rate at which this mRNA is decapped.

The MIE can increase the rate of deadenylation of the PGK1 transcript

In addition to being necessary for rapid decay of the MATα1 transcript the MIE has also been shown to be sufficient to accelerate turnover of the otherwise stable PGK1 transcript (20,21). To determine how the MIE decreases the half-life of the PGK1 mRNA, transcriptional pulse-chase experiments examining the rates of deadenylation and degradation following deadenylation of various PGK1/MATα1 chimeric mRNAs were performed. mRNAs examined were PαP.201–265, PαP.201–351 and PαP.0, which are composed of 65 (the MIE), 150 (the MIE and the following 3′ 85 nt) and 0 nt of MATα1 respectively, inserted in-frame within the PGK1 coding region (20). In good agreement with previous measurements, these transcripts degrade with half-lives of 10, 10 and 29.5 min respectively in the yeast strains used in this study (Table 1; 20).

Transcriptional pulse-chase experiments examining decay of the PαP.201–265, PαP.201–351 and PαP.0 mRNAs indicated that the MIE increased the rate at which the PGK1 mRNA was deadenylated (Fig. 5A–C). The PαP.201–265 and PαP.201–351 mRNAs deadenylated with rates of 6 ± 0.5 and 7 ± 1 nt/min (Fig. 5D and Table 1). In contrast, the PαP.0 mRNA deadenylated at a rate of 3 ± 0.5 nt/min, >2-fold more slowly than the PαP.201–265 and PαP.201–351 mRNAs (Fig. 5D and Table 1). Following deadenylation no significant differences in the rates of decay of these mRNAs were observed (Fig. 5D). However, it could not be concluded that the MIE did not influence the rate at which the PGK1 mRNA was degraded following deadenylation due to the fact that the decay rates measured for the oligo(A) forms of the PαP.201–265 and PαP.201–351 mRNAs (32 and 26 min respectively; Table 1) were greater than the overall decay rates measured for these mRNAs at steady-state. These differences are likely to reflect differences in the rates at which these mRNAs are decapped under the experimental conditions employed in steady-state versus transcriptional pulse-chase experiments. Ultimately, based on the clear differences in the rates of poly(A) shortening between these mRNAs, we conclude that the MIE increases the rate of decay of the PGK1 transcript, at least in part, by increasing the rate at which it is deadenylated. Thus an instability element located in the coding region of an mRNA can effect nucleolytic events that occur at both the 5′- and 3′-ends of an mRNA (see below).

DISCUSSION

The MATα1 mRNA is degraded by deadenylation-dependent mRNA decapping

Two observations strongly suggest that deadenylation precedes degradation of the MATα1 transcript. First, in transcriptional pulse-chase experiments decay of this mRNA occurred following an ~4 min lag during which time the poly(A) tails of some of the mRNA were shortened to an oligo(A) length (Fig. 1A and C). Second, decay products arising from the MMPpG mRNA appeared only once the poly(A) tails of some of the full-length mRNA had been shortened to an oligo(A) length. Furthermore, these decay products had short poly(A) tails, indicating that they were generated from only oligoadenylated full-length mRNA (Fig. 1B and C).

Direct examination of decay of the MATα1 mRNA in yeast mutants lacking either the major decapping or 5′→3′ exonuclease activities indicated that this mRNA is degraded by decapping and 5′→3′ exonucleolytic digestion, since the MATα1 transcript was stabilized roughly 4- and 3-fold respectively in *dcp1*Δ and *xrn1*Δ mutants (Fig. 2). These data, coupled with the previously mentioned evidence for deadenylation preceding the decay of the MATα1 mRNA, strongly support a model in which the MATα1 mRNA is largely degraded by a deadenylation-dependent decapping mechanism. Since the yeast MFA2 and PGK1 transcripts are also degraded through this pathway of mRNA decay (8,17,19) and many additional transcripts are stabilized in either *dcp1*Δ or *xrn1*Δ strains (23,30,34), it is very likely that this is a common pathway of mRNA decay in yeast.

The MIE stimulates mRNA degradation by affecting multiple steps in decay

Our evidence suggests that the MIE can accelerate transcript degradation by stimulating the rates of either deadenylation or mRNA decay following deadenylation. However, the primary affect of the MIE on mRNA turnover depends on the mRNA in which it is contained. For instance, the MIE caused a 2-fold increase in the rate at which the MATα1 and MMPpG mRNAs are decapped (compare Figs 1C and 3C). That the MIE affects decapping rather than 5′→3′ exonucleolytic degradation of these mRNAs comes from the observation that the MATα1.Δ$^{182–339}$ and the MATα1 mRNAs decay with similar kinetics in the absence of Dcp1p (Fig. 4), whereas the MATα1.Δ$^{182–339}$ mRNA is more stable than the MATα1 transcript in the absence of Xrn1p (Fig. 4). Thus, the MIE accelerates decay of the MATα1 and MMPpG mRNAs by increasing the rate at which they are decapped. In contrast, the MIE accelerated degradation of the PGK1 transcript by increasing the rate at which it is deadenylated ~2-fold (Fig. 5).

Why might the primary effect of the MIE on mRNA decay be dependent on the mRNA in which it is located? One possibility is that additional sequences within an mRNA may either antagonize or, alternatively, be redundant to certain functions of the MIE. For instance, given that the MATα1 mRNA becomes only moderately stable ($t_{1/2}$ = 9 min) following a deletion of the MIE it is possible that the MATα1 transcript contains multiple instability elements. These additional elements may stimulate

deadenylation to the same extent as does the MIE. Thus, removal of the MIE from the mRNA would expose only the function that most contributed to degradation of the MATα1 transcript, namely the stimulation of decapping. In contrast, the MIE may not affect decapping of the PGK1 mRNA due to additional features of the PGK1 mRNA that specifically slow decapping. Support for this hypothesis comes from the observation that the 3′-end of the MFA2 mRNA, which is capable of stimulating both deadenylation and decapping of the MFA2 mRNA (7), affects only deadenylation of the PGK1 mRNA (8).

How are translation and mRNA deadenylation and decapping linked?

Several observations strongly suggest that stimulation of mRNA deadenylation and decapping by the MIE is coupled to its translation. The MIE is located in the coding region of the MATα1 mRNA. This location is critical to its function as an instability element, since translation up to or through this element is required for it to promote decay of both the PGK1 (21) and MATα1 transcripts (22). Lastly, the important feature of the 5′ 33 nt of the MIE are a run of rare codons which stimulate decay mediated by the downstream 32 nt (20). These observations, coupled with work presented in this manuscript, suggest a model as to how the MIE functions as an instability element in which ribosomes are required to pause at a run of rare codons positioned just upstream of specific sequences that in turn serve to stimulate mRNA degradation by increasing the rates of either mRNA deadenylation or decapping. How translation and mRNA deadenylation and decapping can be coupled is unclear (see below), however, there are several additional examples of translation affecting mRNA deadenylation. Deadenylation, but not degradation following deadenylation, of the unstable mammalian c-*myc* mRNA is slowed when cells are treated with translation inhibitors (35). Similarly, insertion of a hairpin that blocks translation in *cis* into the 5′-UTR of an mRNA destabilized by the presence of the c-*fos* coding region determinant of instability (CRDI) negates the rapid deadenylation promoted by this element (36). Thus the coupling of translation and mRNA deadenylation may be common to many eukaryotic transcripts. Determining how this coupling is achieved will increase our understanding of mRNA turnover in general.

How do sequence elements influence deadenylation and decapping?

There are now several examples of RNA sequences and structures that affect decay through the deadenylation-dependent decapping pathway. These include the MIE (this paper), the 3′-UTR of the unstable MFA2 mRNA (7) and strong secondary structures such as a poly(G) tract and a stem–loop structure, which when inserted into the PGK1 5′-UTR can accelerate deadenylation and decapping (9). Similarly, instability elements have been identified in both the coding region and 3′-UTR of the unstable mammalian c-*fos* mRNA which increase both the rate at which mRNAs are deadenylated and degraded following deadenylation (6), although the mode of degradation following deadenylation is not known. One interesting question is why instability elements that consistently influence only one step in degradation (i.e. either deadenylation or decay following deadenylation) have not been identified.

Two general models may explain why sequence elements so far identified are capable of affecting both deadenylation and mRNA degradation following deadenylation. In one view, sequence elements may often contain overlapping, but separate, elements that influence different steps in mRNA degradation. Support for this model comes from the observation that specific point mutations in the AUUUA motif and/or accompanying U-rich region from the unstable c-*fos* mRNA affect the ability of this instability element to influence either deadenylation or mRNA degradation following deadenylation (6,9). Similarly, specific mutations in the 3′-UTR of the yeast MFA2 mRNA can primarily affect the ability of this portion of the mRNA to stimulate either deadenylation or decapping (7).

A second model is based on observations that suggest an interaction between the 5′- and 3′-termini of an mRNA may be central to the control of mRNA decay. These observations include the fact that the poly(A) tail–Pab1p complex serves as an inhibitor of mRNA decapping (37) and that sequences in the 3′-UTR of the MFA2 mRNA can influence mRNA decay following deadenylation (7). In this model a mRNP structure involving the 5′- and 3′-ends of an mRNA would control rates of both deadenylation and decapping. This mRNP structure would in turn be influenced by signals received from specific elements within an mRNA, such as the MIE, and respond by changing rates of deadenylation, decapping or both. In this view the mRNP structure would serve to integrate the specific inputs received from different elements within an mRNA. In addition, because the mRNP structure affects both deadenylation and decapping, the specific elements that influence it would be capable of influencing both of these processes. This model is attractive because it provides an explanation for how sequences located in the coding region of an mRNA are able to influence nucleolytic events at both the 5′- and 3′-ends of an mRNA, since the element need only affect a central mRNP structure rather than the actual nucleolytic events themselves. Ultimately, identification of the specific *trans*-acting factors that mediate the effects of instability elements and determination of whether these factors directly or indirectly impact the deadenylation and decapping machinery will facilitate an understanding of how the decay of individual mRNA half-lives is controlled.

REFERENCES

1 Hargrove,J.L. and Schmidt,F.H. (1989) *FASEB J.*, **3**, 2360–2370.
2 Belasco,J. and Brawerman,G. (1993) *Control of Messenger RNA Stability.* Academic Press, San Diego, CA.
3 Beelman,C.A. and Parker,R. (1995) *Cell*, **81**, 179–183.
4 Ross,J. (1995) *Microbiol. Rev.*, **59**, 423–450.
5 Wilson,T. and Triesman,R. (1988) *Nature*, **336**, 396–399.
6 Shyu,A.B., Belasco,J.G. and Greenberg,M.E. (1991) *Genes Dev.*, **5**, 221–234.
7 Muhlrad,D. and Parker,R. (1992) *Genes Dev.*, **6**, 2100–2111.
8 Decker,C.J. and Parker,R. (1993) *Genes Dev.*, **7**, 1632–1643.
9 Chen,C.-Y.A., Chen,T.-M. and Shyu,A.-B. (1994) *Mol. Cell. Biol.*, **14**, 416–426.
10 Lagnado,C.A., Brown,C.Y. and Goodall,G.J. (1994) *Mol. Cell. Biol.*, **14**, 7984–7995.
11 Zubiaga,A.M., Belasco,J.G. and Greenberg,M.E. (1995) *Mol. Cell. Biol.*, **15**, 2219–2230.
12 Brown,B. and Harland,R. (1990) *Genes Dev.*, **4**, 1925–1935.
13 Brown,B.D., Zipkin,I.D. and Harland,R.M. (1993) *Genes Dev.*, **7**, 1620–1631.
14 Bernstein,P.L., Herrick,D.J., Prokipcak,R.D. and Ross,J. (1992) *Genes Dev.*, **6**, 642–654.
15 Nielsen,F.C. and Christiansen,J. (1992) *J. Biol. Chem.*, **267**, 19404–19411.
16 Binder,R. *et al.* (1994) *EMBO J.*, **13**, 1969–1980.
17 Muhlrad,D., Decker,C.J. and Parker,R. (1994) *Genes Dev.*, **8**, 855–866.

18 Muhlrad,D. and Parker,R. (1994) *Nature*, **370**, 578–581.
19 Muhlrad,D., Decker,C.J. and Parker,R. (1995) *Mol. Cell. Biol.*, **15**, 2145–2156.
20 Caponigro,G., Muhlrad,D. and Parker,R. (1993) *Mol. Cell. Biol.*, **13**, 5141–5148.
21 Parker,R. and Jacobson,A. (1990) *Proc. Natl. Acad. Sci. USA*, **87**, 2780–2784.
22 Hennigan,A. and Jacobson,A. (1996) *Mol. Cell. Biol.*, **16**, 3833–3843.
23 Beelman,C.A. *et al.* (1996) *Nature*, **382**, 642–646.
24 Chen,C.Y.A. and Shyu,A.B. (1994) *Mol. Cell. Biol.*, **14**, 8471–8482.
25 Zimmerman,S.B., Cohen,S.H. and Davies,D.R. (1975) *J. Mol. Biol.*, **92**, 181–192.
26 Williamson,J.R., Raghuraman,M.K. and Cech,T.R. (1989) *Cell*, **59**, 871–880.
27 Stevens,A. and Poole,T.L. (1995) *J. Biol. Chem.*, **270**, 16063–16069.
28 Vreken,P. and Raue',H. A. (1992) *Mol. Cell. Biol.*, **12**, 2986–2996.
29 Stevens,A. (1978) *Biochem. Biophys. Res. Commun.*, **81**, 656–661.
30 Larimer,F.W. and Stevens,A. (1990) *Gene*, **95**, 85–90.
31 Heyer,W.D., Johnson,A.W., Reinhart,U. and Kolodner,R.D. (1995) *Mol. Cell. Biol.*, **15**, 2728–2736.
32 Amberg,D.C., Goldstein,A.L. and Cole,C.N. (1992) *Genes Dev.*, **6**, 1173–1189.
33 Kenna,M., Stevens,A., McCammon,M. and Douglas,M.G. (1993) *Mol. Cell. Biol.*, **13**, 341–350.
34 Hsu,C.L. and Stevens,A. (1993) *Mol. Cell. Biol.*, **13**, 4826–4835.
35 Laird-Offringa,I.A., de Wit,C.L., Elfferich,P. and van der Eb,A.J. (1990) *Mol. Cell. Biol.*, **10**, 6132–6140.
36 Schiavi,S.C. *et al.* (1994) *J. Biol. Chem.*, **269**, 3441–3448.
37 Caponigro,G. and Parker,R. (1995) *Genes Dev.*, **9**, 2421–2432.